Int. J.Nano Dimens. 5(4): 329-335, Autumn 2014
ISSN: 2008-8868

Contents list available at **IJND**

International Journal of Nano Dimension

Journal homepage: *www.IJND.ir*

A visible light driven doped TiO_2 nanophotocatalyst: Preparation and characterization

S. M. E. Zakeri[1]
M. Asghari[1, 2, *]
M. Feilizadeh[3]
M. Vosoughi[3]

[1]*Separation Processes Research Group (SPRG), Department of Engineering, University of Kashan, Kashan, Iran.*
[2]*Energy Research Institute, University of Kashan, Ghotb-e-Ravandi Ave., Kashan, Iran.*
[3]*Chemical and petroleum Engineering Deportment, Sharif University of Technology, Tehran, Iran.*

Received 21 February 2013
Received in revised form
02 May 2013
Accepted 17 May 2013

* Corresponding author:
M. Asghari
Energy Research Institute,
University of Kashan, Ghotb-e-Ravandi Ave., Kashan, Iran.
Tel +98 361 591 2427
Fax +98 361 591 2424
Email asghari@kashanu.ac.ir

ABSTRACT

A useful nanophotocatalyst (La,S-TiO_2) was prepared by a sol-gel method and characterized by UV–vis diffuse reflectance spectroscopy (DRS), X-ray diffraction (XRD), photoluminescence emission spectroscopy (PL) and scanning electron microscopy (FESEM). The results showed that the La,S-TiO_2, which calcined at 550 °C, contained only anatase phase and its crystal size was 23 nm. In addition, the FESEM analysis indicates that the La,S-TiO_2 nano particles with diameter of 20 to 25 nm could have a good dispersion in solution. In order to evaluate of activity of the modified synthesized photocatalyst (La,S-TiO_2), comparison between modified synthesized TiO_2 (La,S-TiO_2) and pure synthesized TiO_2 for degradation of Methyl Orange was investigated. It was found that the modified synthesized photocatalysis (La,S-TiO_2) has much higher photocatalytic activity than undoped TiO_2 for the degradation of contamination.

Keywords: *Nanophotocatalyst; La,S-TiO_2; Methyl orange; Contamination; Synthesized; Sol-gel method.*

INTRODUCTION

Photocatalysis has recently become a common word and various products using photocatalytic functions have been commercialized. Among many candidates for photocatalysts, TiO_2 is almost the only material suitable for industrial use at present and also probably in the future. Because, TiO_2 is a high efficient, low cost as well as high stable photocatalysis and also its photogenerated holes are highly oxidizing. In addition, the photogenerated electrons are reducing enough to produce superoxide from oxygen [1,2].

Advanced oxidation processes (AOPs) have received great attention for treatment of contaminated water. The mechanism of degradation in AOPs is based on the formation of a very reactive hydroxyl radical (OH•) which can oxidize a wide range of organic compounds [3, 4].

The photocatalytic treatment is one of the most efficient and economical AOPs for elimination of hazardous environmental pollutants using TiO_2 [5-7]. However, most of researchers have worked under UV irradiation due to the band edge absorption threshold less than 400 nm (wide band gap: 3.2 ev) of TiO_2 [8-11]. Doping TiO_2 with metals cause enhancements of adsorbed visible light. Recently, doping lanthanide metals such as La, Eu and Ce has received much attention [12-14]. Among various dopants, the lanthanide element doped in TiO_2 has special 4f electronic structure. This metal can form complexes with different Lewis bases in the inter-action of the functional groups with their *f*-orbital and improve conversion efficiency of TiO_2 [15]. Many researchers have reported that doping with La exhibits effective photocatalytic activity for the degradation of organic pollutants under visible light irradiation [16-19]. On the other hand, it appears that doping with S makes an enormous improvement in the performance of TiO_2 photocatalyst [20,21]. Doping of sulfur could help to form a new band gap, decrease crystallite size and control the crystallization [22,23]. Wang et al. [24] reported that doping of S causes 48% increase in removal efficiency of L-acid under visible light in comparison with pure TiO_2 without sulfur doping.

In this article, La,S-TiO_2 and pure TiO_2 nanoparticle photocatalysts were synthesized using a sol–gel process. Moreover, the photocatalysis was utilized to degrade the Methyl Orange (Figure 1) in order to evaluate the activity of the modified synthesized photocatalyst (La,S-TiO_2) in visible light irradiation.

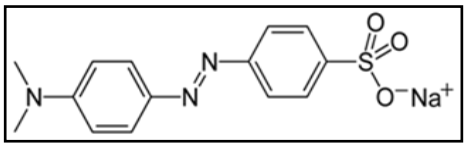

Fig. 1. Structure of Methyl Orange

EXPERIMENTAL

Catalyst preparation

All chemicals used in this study were reagent-grade without further purification. La,S-TiO_2 precursor was prepared by a sol–gel process as follows: first, Titanium (IV) isopropoxide was dissolved and hydrolyzed in glacial acetic acid at a mole ratio of 1:10 at 0 ˚C. The solution was stirred magnetically for 30 min to give solution 1. $La(NO_3)3.6H_2O$ (La:Ti mol ratio = 0.3%) and thiourea (S:Ti =1 molar ratio) was dissolved in appropriate amount of deionized water to give solution 2. Then the solution 1 was added dropwise to the solution 2 for 70 min while solution 2 mixing. The resulting solution was ultrasonicated at 0 ˚C for 20 min and stirred continuously for 260 min. Subsequently, the solution was ultrasonicated for second time and kept for a day at room temperature in dark area. Then the solution was gelated at 76 °C and dried at 120 °C. The dried photocatalyst was ground with a mortar and pestle into fine powders and calcined at 550 °C for 3 h to prepare the coveted nanoparticle photocatalysts. Undoped TiO_2 was synthesized similar to above method, without using of $La(NO_3)3.6H_2O$ and thiourea in solution 2.

Characterization of synthesized photocatalysts

The phases present in the photocatalyst was investigated using X-ray diffraction (XRD) patterns (Philips X'pert Pro MPD model) with Cu Kradiation (40 kV, 40 mA) at 2angles from 10° to 80° and with a scan speed of 4° min^{-1}. The structure, surface characteristics and size of nanoparticle was investigated by using FESEM (Field Emission Scanning Electron Microscope) Hitachi S4160. UV-Vis spectroscopy of the samples was taken out by an Ava Spec-2048TEC spectrometer from 350 nm to 750 nm wavelengths. .As also, the photoluminescence (PL) spectra of the samples were recorded by a Cary Eclipse fluorescence spectrometer at room temperature. The degradation efficiency was measured by UV-Vis spectrophotometer (Perkin Elmer Lambda2S).

Evaluation of photocatalytic activity

The photo colorization experiments were performed in a Pyrex glass 100 ml (10 ppm) of Methyl Orange solution and 100 mg of certain photocatalyst. The photoreactor temperature was kept at room and pH of solution was constant (pH=3). A 400 W Osram lamp equipped with a UV cut-off filters (λ> 400 nm) was employed as a visible light source. The mixture was magnetically stirred in the darkness for 30 min in order to reach

the steady state of adsorption equilibrium on the nanophotocatalyst surface. After that the lamps turned on and performed during 90 min. Then, the sample was centrifuged to extract solid particles. Remain solution used for analysis. The Methyl Orange concentration in the solution was determined by using a UV spectrophotometer. Their photocatalytic degradation efficiency can be calculated by formula: $D= ((A_0-A)/A_0) \times 100\%$, in which A_0 is the initial absorption and A is the absorption at the time.

RESULTS AND DISCUSSION

XRD

Figure 2 shows XRD patterns of La,S-TiO_2 and undoped TiO_2. The strongest peak at $2\theta = 25.48^{\circ}$ clearly demonstrates the (101) anatase phase of TiO_2 crystal. No observable rutile phase is observed in both samples. The phase structures were affected by lanthanum doping. In addition to this, the La phase could observe in the pattern. This maybe indicated that La^{3+} entered into TiO_2 crystal lattice to substitute for Ti^{4+} [25,26]. Moreover, Crystallite sizes of the prepared samples were determined through the widths of half-height in terms of the Scherrer equation:

$$Crystallite\ size = \frac{0.89\,\lambda}{W\cos\theta} \qquad (1)$$

Where λ is the X-ray wavelength corresponding to Cu-Kα radiation (λ = 0.15406 nm), $W = W_b - W_s$, W_b is the broadened profile width of the experimental sample and W_s is the standard profile width of the reference sample, and θ is the diffraction angle with characteristic peak [27].

The values of crystallite size of undoped TiO_2 and La,S-TiO_2 are 36 and 23 nm, respectively. Based on the XRD analyses, La^{3+} & S^{+6} doping can hinder the increase of the crystallite size, which can result in the higher photocatalytic activity of the TiO_2 sample.

FESEM

Figure 3 shows FESEM micrograph of the La,S-TiO_2 calcined at 550 °C. The grains are found to be uniform, with diameter from 20 to 25 nm, which indicates that the sample could have good dispersion in solution. The result was in accordance with the value determined by XRD (23 nm).

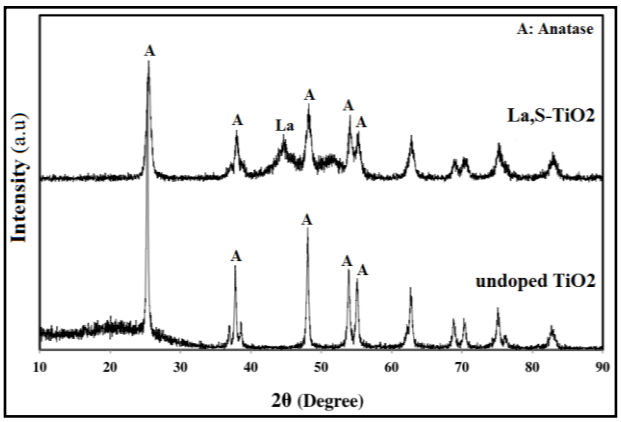

Fig. 2. XRD patterns of undoped TiO_2 and 0.3% La,S-TiO_2 nanoparticles

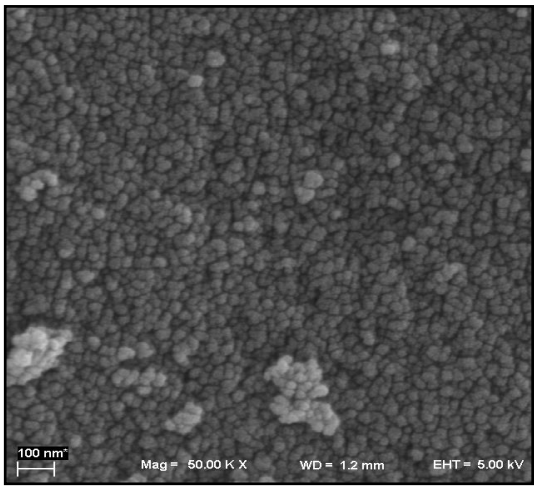

Fig. 3. FSEM image of La,S-TiO_2

DSR

The results of UV–vis Diffuse Reflectance Spectra (DRS) analysis of the prepared samples are illustrated in Figure 4. The absorption spectrum of the La,S-TiO_2 sample showed a stronger absorption in visible light region and a red shift in the adsorption edge. The red shift may be ascribed to that the doped sulfur atoms could narrow the band gap of TiO_2 due to the hybridization of S3p with O2p from oxygen [28]. The doping of La could separate the electron–hole

pairs effectively and increase the response region of visible-light [29]. As a result, the synergism effect of rare earth metal ions and sulfur into TiO_2 could shift its optical absorption edge from UV into visible light range [30].

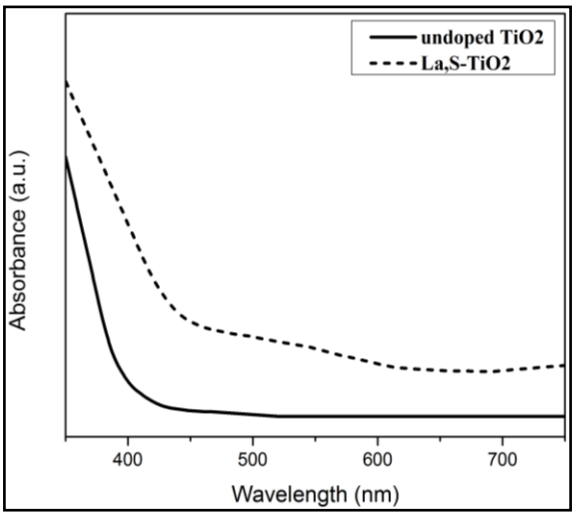

Fig. 4. Optical absorbance of undoped TiO_2 and La,S-TiO_2 nanoparticles

PL

The PL emission spectra of the pure and La,S-TiO_2 are shown in Figure 5. It can be seen that the PL intensities of La,S-TiO_2 is lower than undoped TiO_2. As the PL emission results from the recombination of photo-induced electron–hole pairs, the lower PL intensity means the lower recombination rate of electron–hole pairs and higher photocatalytic activity [31,32].

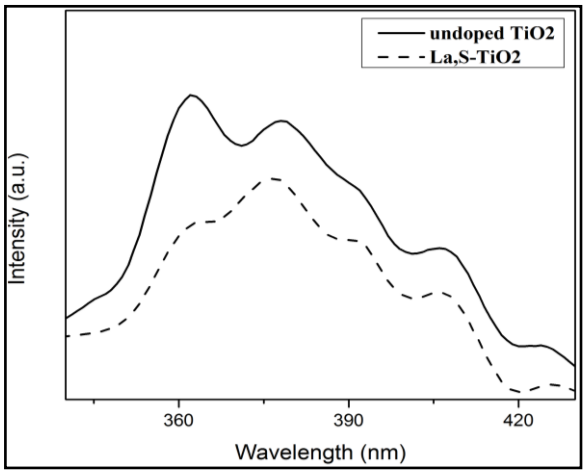

Fig. 5. PL spectra of TiO_2 and La,S-TiO_2 nanophotocatalysts

Photocatalytic activities

The photocatalytic activities of the prepared samples were measured for degradation of ecologically abundant dye Methyl Orange (MO) in water under visible-light irradiation. Figure 6 represents the percent of contamination degradation with pure TiO_2 and La,S-TiO_2. Compared to the pure TiO_2, the modified photocatalysts showed a significant increase in the MO photodegradation rates. On the other hands, the figure shows that La,S-TiO_2 is about 2 times more active than undoped TiO_2 during degradation of MO under visible light. This behavior could be explained by the effect of La and S as dopants. They can operate as electron traps, increasing the electron–hole separation and the subsequent transfer of the trapped electron to the adsorbed O_2 acting as an electron acceptor [33]. In addition, the doping causes a decrease in particle size and an increase in specific surface area of photocatalyst nano particles.

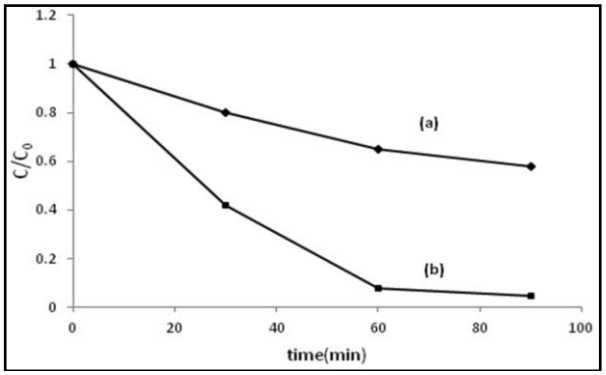

Fig. 6. Photocatalytic degradation using pure (a) TiO_2 and (b) La,S-TiO_2.

Moreover, photocatalytic reactions kinetics on photocatalyst can be expressed by the Langmuir–Hinshelwood (L–H) model [34].When the initial concentration of dye is low enough (like in this work that the maximum dye concentration is only 10 ppm), the reaction rate can be expressed as follow [35]:

$$\ln(\frac{C_t}{C_0}) = -K_{app}t \qquad (2)$$

Where C_0 and C_t are dye concentrations at zero time and time t, respectively, and, k_{app} is the

experimental photocatalytic pseudo-first order rate constant.

The kinetic curves for the degradation of the aqueous solution of the Methyl Orange (10 ppm) with TiO_2 (1g/l) and La,S-TiO_2 (1g/l) are shown in Figure 7. These follow pseudo first order kinetics as confirmed by the linear transform $\ln(C_t/C_0) = -K_{app}t$. The apparent rate constants calculated from the above curves were as follows:

With La,S/TiO_2, K_{app}= 0.0363(min^{-1}) and R^2= 0.964
With TiO_2, K_{app} = 0.0061(min^{-1}) and R^2 = 0.981

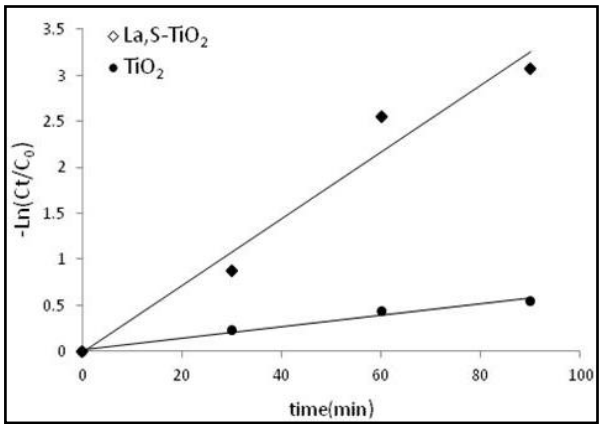

Fig. 7. Kinetic analysis with La,S TiO_2 and TiO_2

CONCLUSIONS

The pure TiO_2 and La,S-TiO_2 nanoparticles were prepared by sol-gel method. The XRD pattern of La,S-TiO_2 and pure TiO_2 shows anatase the crystal size were about 36 and 23 nm, respectively. The FESEM photograph shows spherical particles with the average size of 23 nm. In contrast to undoped TiO_2, La,S-TiO_2 sample shows a strong absorption in the visible light region and a red shift in the adsorption edge. La,S-TiO_2 is about 2 times more active than undoped TiO_2 during degradation of MO under visible light.

ACKNOWLEDGMENTS

The authors are grateful to the Energy Research Institute at University of Kashan for supporting this work.

REFERENCES

[1] Hashimoto K., Irie H., Fujishima A., (2005), TiO_2 Photocatalysis: A Historical Overview. Future Prospects. *Jap. J. Appl. Phys.* 44: 8269–8285.

[2] Fujishima A., Rao T. N., Tryk D. A., (2000), Titanium dioxide photocatalysis, *J. Photochem. Photobio. C: Photochem. Rev.*1: 1–21.

[3] Badawy M. I., Ghaly M. Y., Gad-Allah T. A., (2006), Advanced oxidation processes for the removal of organophosphorus pesticides from wastewater, *Desalination*. 194: 166–175.

[4] Vilhunen S., Sillanpää M., (2010), Recent developments in photochemical and chemical AOPs in water treatment: a mini-review. *Rev. Env. Sci. Biotechnol.* 9: 323–330.

[5] Giri R. R., Ozaki H., Ota S., Taniguchi S., Takanami R., (2010), Influence of inorganic solids on photocatalytic oxidation of 2,4-dichlorophenoxy acetic acid with UV and TiO_2 fiber in aqueous solution, *Desalination*. 255: 9-14.

[6] Borker P., Salker A. V., (2006), Photocatalytic degradation of textile azo dye over Ce1−xSnxO_2 series. *Mater. Sci. Eng. B.* 133: 55–60.

[7] Tizaoui C., Mezughi K., Bickley R., (2011), Heterogeneous photocatalytic removal of the herbicide clopyralid and its comparison with UV/H_2O_2 and ozone oxidation techniques. *Desalination*. 273: 197–204.

[8] Cantaveneraa M. J., Catanzaro I., Loddo V., Palmisano L., Sciandrello G., (2007), Photocatalytic degradation of paraquat and genotoxicity of its intermediate products, *J. Photochem. Photobio. A: Chem.* 185: 277–282.

[9] Lin C., Lin K., (2007), Photocatalytic oxidation of toxic organohalides with

TiO_2/UV: The effects of humic substances and organic mixtures. *Chemosphere*. 66: 1872-1877.

[10] Florêncio M. H. , Pires E., Castro A. L., Nunes M. R., Borges C., Costa F. M., (2004), Photodegradation of Diquat and Paraquat in aqueous solutions by titanium dioxide: evolution of degradation reactions and characterisation of intermediates. *Chemosphere*. 55: 345–355.

[11] Pourata R., Khataee A. R., Aber S., Daneshvar N., (2009), Removal of the herbicide Bentazon from contaminated water in the presence of synthesized nanocrystalline TiO_2 powders under irradiation of UV-C light. *Desalination*. 249: 301–307.

[12] Li L., Zhuang H., Bu D., (2011), Characterization and activity of visible-light-driven TiO_2 photocatalyst codoped with lanthanum and iodine, *App. Surf. Sci.* 257: 9221– 9225.

[13] Wang P., Cao M., Ao Y., Wang C., Hou J., Qian J., (2011), Investigation on Ce-doped TiO_2-coated BDD composite electrode with high photoelectrocatalytic activity under visible light irradiation,. *Electrochem. Comm.* 13: 1423–1426.

[14] Ramya S., Nithila S. D. R., George R. P., Krishna D. N. G., Thinaharan C., Kamachi, U., (2013), Antibacterial studies on Eu–Ag codoped TiO_2 surfaces. *Ceram. Int.* 39: 1695–1705.

[15] Cao G. X., Li Y. G., Zhang Q. H., Wang H. Z., (2010), Enhanced Visible Light-Driven Photocatalytic Performance of La-Doped TiO_2−xFx, *J. Am. Ceram. Soc*. 93: 25-27.

[16] Liqiang J., Xiaojun S., Baifu X., Baiqi W., Weimin C., Hongganga F., (2004), The preparation and characterization of La doped TiO_2 nanoparticles and their photocatalytic activity. *J. Sol. Stat. Chem.* 177: 3375-3382.

[17] Zhao N., Yao M., Li F., Lou F. P., (2011), Microstructures and photocatalytic properties of Ag^+ and La^{3+} surface codoped TiO_2 films prepared by sol–gel method. *J. Sol. Stat. Chem.* 184: 2770–2775.

[18] Andoa T., Wakamatsua T., Masudaa K., Yoshidaa N., Suzukia K, Masutanib K. S., Katayamab I., Uchidab H., Hiroseb H., Kamimotob A., (2009), Photocatalytic behavior of heavy La-doped TiO_2 films deposited by pulsed laser deposition using non-sintered target. *Appl. Surf. Sci.* 255: 9688-9690.

[19] Wu X. H., Ding X. B., Qin W., He W. D., Jiang Z. H., (2006), Enhanced photo-catalytic activity of TiO_2 films with doped La prepared by micro-plasma oxidation method. *J. Hazard. Mater.* 137: 192-197.

[20] Bidaye P. P., Khushalani D., Fernandes J. B., (2010), A simple method for synthesis of S-doped TiO_2 of high photocatalytic activity. *Catal. Lett.* 134: 169-174.

[21] Dozzi M. V., Livraghi S., Giamello E., Selli E., (2011), Photocatalytic activity of S- and F-doped TiO_2 in formic acid mineralization. *Photochem. Photobio. Sci.* 10: 343-349.

[22] Yamazaki S., Fujinaga N., Araki K., (2001), Effect of sulfate ions for sol–gel synthesis of titania photocatalyst. *App. Catal. A: Gen.* 210: 97–102.

[23] Takeshita K., Yamakata A., Ishibashi T., Onishi H., Nishijima K., Ohno T., (2006), Transient IR absorption study of charge carriers photogenerated in sulfur-doped TiO_2. *J. Photoche. Photobio A: Chem.* 177: 269–275.

[24] Wanga Y., Li J., Peng P., Lu T., Wang L., (2008), Preparation of S-TiO_2 photocatalyst and photodegradation of L-acid under visible light. *App. Surf. Sci*. 254: 5276–5280.

[25] Ghorai T. K., Biswas S. K., Pramanik P., (2008), Photooxidation of different organic

dyes (RB, MO, TB, and BG) using Fe(III)-doped TiO_2 nanophotocatalyst prepared by novel chemical method. *Appl. Surf. Sci*. 254: 7498–7504.

[26] Zhu J., Zheng W., He B., Zhang J., Anpo M., (2004)., Characterization of Fe-TiO_2 photocatalysts synthesized by hydrothermal method and their photocatalytic reactivity for photodegradation of XRG dye diluted in water. *J. Mol. Catal. A: Chem*. 216: 35-43.

[27] Tayade R. J., Kulkarni R. G., Jasra R.V., (2006), Photocatalytic Degradation of Aqueous Nitrobenzene by Nanocrystalline TiO_2. *Ind. Eng. Chem*., 45: 922-927.

[28] Umebayashi T., Yamaki T., Tanaka S., Asai K., (2003), Visible Light-induced Degradation of Methylene Blue on S-doped TiO_2. *J. Chem. Lett*. 32: 330-331.

[29] Cen J. W., Li X. J., He M. X., (2005), Effects of La^{3+} Non-uniformly Doping in TiO_2 Films on Photocatalytic Activities. *J. Rare Earth Soc*. 23: 668-673.

[30] Xu K., Zhu G., (2009), Preparation and characterization of nano-La (S, C)-TiO_2 oriented films by template hydrothermal synthesis. *Appl. Sur. Sci*. 255: 6691–6695.

[31] Wu Y., Liu H., Zhang J., Chen F., (2009), Enhanced Photocatalytic Activity of Nitrogen-Doped Titania by Deposited with Gold. *J. Phys. Chem*. C. 113: 14689–14695.

[32] Gao B., Ma Y., Cao Y., Yang W., Yao J., (2006), Great enhancement of photocatalytic activity of nitrogen-doped titania by coupling with tungsten oxide, *J. Phys. Chem. B*. 110: 14391–14397.

[33] Serpone N., Lawless D., (1994), Spectroscopic, Photoconductivity, and Photocatalytic Studies of TiO_2 Colloids: Naked and with the Lattice Doped with Cr^{3+}, Fe^{3+}, and V^{5+} Cations. *Langm*., 10: 643-652.

[34] Wahi R. K., Yu W. W., Liu Y., Mejia M. L., Falkner J. C., Nolte W., Colvin V. L., (2005), Photodegradation of Congo Red catalyzed by nanosized TiO_2. *J. Mol. Catal. A: Chem.* 242: 48–56.

[35] Kaur S., Singh V., (2007), TiO_2 mediated photocatalytic degradation studies of Reactive Red 198 by UV irradiation. *J. Hazard. Mater*. 141: 230–236.

Cite this article as: S. M. E. Zakeri *et al.*: A visible light driven doped TiO_2 nanophotocatalyst: preparation and characterization.
Int. J.Nano Dimens. 5(4): 329-335, Autumn 2014